Am J Transl Res 2018;10(5):1431-1443
www.ajtr.org /ISSN:1943-8141/AJTR0066825

Original Article

Synergistic effect of a LPEMF and SPIONs on BMMSC proliferation, directional migration, and osteoblastogenesis

Shaoyu Wu[1], Qiang Yu[2], Yang Sun[1], Jing Tian[2]

[1]Zhujiang Hospital of Southern Medical University, Guangzhou 510282, Guangdong, PR China; [2]Department of Orthopaedics, Zhujiang Hospital, Southern Medical University, Guanzhou 510280, Guangdong, PR China

Received October 9, 2017; Accepted April 19, 2018; Epub May 15, 2018; Published May 30, 2018

Abstract: Pulsed electromagnetic fields (PEMFs) represent a new type of physiotherapy that has been shown to be effective for improving bone fracture healing and treating osteoporosis. Targeted therapy with bone marrow mesenchymal stem cells (BMMSCs) has been the focus of several recent studies. The key to such therapy is the effective application of certain nanomaterials in BMMSCs so they achieve an ideal target concentration under the influence of a PEMF. In our present study, the effects of a PEMF on the process of osteoblastogenesis were systematically investigated using superparamagnetic iron oxide nanoparticle (SPION)-labeled BMMSCs. Rat BMMSCs labeled with SPIONs were exposed to a low-frequency pulsed electromagnetic field (LPEMF) of 50 Hz at 1.1 mT. Exposure to the LPEMF resulted in an enhanced proliferation of SPION-labeled BMMSCs when compared with a control group. Furthermore, observations made by transmission electron microscopy (TEM) revealed greater cell concentrations in the central zone with exposure to the LPEMF than in the peripheral zone without LPEMF stimulation, indicating that a LPEMF could induce the migration of SPION-labeled BMMSCs towards a magnetic field. Transwell experiments confirmed that combining SPIONs with a LPEMF could significantly promote the directional migration of BMMSCs. Von Kossa and ALP staining of LPEMF-exposed SPION-labeled cells was more intense, and those cells displayed higher levels of ALP activity than control cells. The SPION-labeled, LPEMF-exposed cells also showed increased levels of osteogenesis-related gene and protein expression (e.g., ALP, OCN, and RUNX2) in PCR and western blot studies. Taken together, our findings suggest that a combination of LPEMF and SPIONs exerts a synergistic effect on promoting the directional migration and osteogenic differentiation of BMMSCs, indicating that application of a LPEMF in conjunction with SPIONs may constitute a method for treating bone defects.

Keywords: Pulsed electromagnetic fields, bone marrow mesenchymal stem cells, superparamagnetic iron oxide nanoparticles, osteoblastogenesis

Introduction

With the arrival of an aging society, bone defects have become one of the most common disorders among older people. Decreases in bone mass accompanied by bone micro-structure deterioration can lead to several systemic bone disorders, including osteoporosis and pathologic bone fracture [1]. Conventional pharmacologic agents (e.g. calcitonin, estrogen, growth hormone, and bisphosphonates) either promote bone formation or inhibit bone resorption, and have a long history of use in treating osteopenia [2]. Nevertheless, the long-term effects of these agents have not been fully elucidated, and the disease recurrence rate is high, which has limited their further application [3, 4]. During the past decade, stem cell therapies and tissue engineering have been introduced as methods for treating bone defects, but due to a deficiency of materials and the risk for carcinogenicity, only a few of these treatment strategies are currently available. Therefore, it is very important to identify safer and more effective methods for preventing and treating bone defects.

Pulsed electromagnetic field (PEMF) therapy was first used to treat bone fractures by Basset et al. [5] in 1974, and since that time, the under-

ling therapeutic mechanism of PEMF therapy has received increased attention from scientists. Substantial evidence indicates that as a noninvasive method, PEMF therapy exerts biological effects on a variety of bone defects and diseases, ranging from bone fractures to osteoporosis [6]. Previous studies showed that PEMF exposure is capable of improving skeletal biomechanical strength and enhancing bone mineralization [7]. Subsequent studies have shown that a PEMF with a specific frequency and intensity can promote the proliferation and differentiation of osteoblast precursors. Chang et al. [8] discovered that a PEMF of 15 Hz at 7 mT could significantly promote osteoblast production. Tsai et al. [9] showed that a PEMP of 15.38 Hz at 0.1 mT could improve the proliferation and differentiation of osteoblasts. Diniz et al. [10], reported that a PEMF of 7 Hz at 0.13 mT was capable of increasing the percentage of proliferating osteoblasts, while a PEMF of 7.5 Hz at 0.32 mT attenuated cell proliferation. In spite of these gratifying results, the potential effect of a PEMF on osteoblastogenesis and the mechanism by which a PEMF influences mesenchymal stem cell proliferation and differentiation have remained poorly understood, which limits the further clinical application of PEMF therapy.

Targeted therapy with stem cells has enabled the use of new strategies for treating disease. When compared with pharmacologic treatments, targeted stem cell therapy has no dose-toxicity effect [11]. Stem cells can also differentiate and then secrete cytokines [12, 13]. Traditional targeted stem cell therapies can only concentrate stem cells or force them to maintain their characteristics to limited extent. The low targeting efficiency and concentrations of stem cells in target organs and tissues have impeded research and the further clinical application of stem cell therapy. Bone marrow mesenchymal stem cells (BMMSCs) can differentiate into osteoblasts, chondrocytes, neurons, and other cell types [14]. They can express osteogenic factors and angiogenin [15], which account for their direct effect on osteogenesis. Superparamagnetic iron oxide nanoparticles (SPIONs) possess a net zero magnetization value at room temperature (~25°C), and because of their high thermal stability, low toxicity and superparamagnetism [16], have be used in the fields of biomedicine and biotechnology [17]. Moreover, magnetic nanoparticles can achieve a targeted migration toward an external magnetic field [18, 19]. It has been suggested that a magnetic field might activate the superparamagnetism of SPIONs and promote the differentiation of bone progenitor cells into osteoblasts [20]. Previously, we developed a new type of SPION with a 12 nm diameter. These SPIONs are biologically stable and can be monodispersed. Moreover, following surface modification, these new SPIONs maintain their stability in cell culture medium [21].

We hypothesized that a low-frequency pulsed electromagnetic field (LPEMF) might induce the directional migration of SPION-labeled BMMSCs and activate the superparamagnetism of SPIONs, resulting in increased cell proliferation and the promotion of osteogenic differentiation. To test our hypothesis, we labeled BMMSCs with an appropriate concentration of SPIONs, and then applied a LPEMF to the cells to investigate the synergistic effect of a PEMF and SPIONs on osteoblastogenesis. In addition, cell migration and the concentration of SPION-labeled BMMSCs migrating toward a specific target were examined during the process of PEMF-stimulated-osteogenesis.

Materials and methods

Cell culture and purification

All animals were maintained in accordance with Institutional Animal Care and Use Guidelines, and the experimental protocols were approved by the Animal Experiments Committee of Southern Medical University (Permit Number: 20163291). Wistar rats (2-4 weeks old; 90-120 g) were anesthetized, and their tibias and fibulas were dissected after disinfection. The bone marrow was repeatedly flushed out with Dulbecco's modified Eagle's medium (DMEM)/F-12 (Gibco, Waltham, MA, USA) and then centrifuged at 1000 rpm for 10 min. The resulting pellet was collected and re-suspended in DMEM/F-12 containing 10% fetal bovine serum (FBS; Gibco) and 1% penicillin-streptomycin (Gibco) in a 25-cm^2 culture flask, which was then placed in a 37°C humidified incubator with a 5% CO_2 atmosphere. Approximately 10 days later, cells filled the bottom of the culture bottles, and those cells were designated as the first cell culture passage. The cells were then

sub-passaged at a 1:1 ratio, amplified, purified, and expanded to third-passage cells. The third-passage BMMSCs were digested and prepared as single cell suspensions in 100 μL of PBS and kept shielded from light. Next, the culture medium and non-adherent cells were removed. The harvested cells were confirmed as BMSCs by flow cytometry performed using FITC-conjugated rat anti-mouse CD34 (2.5 μL), CD45 (0.625 μL), CD90 (0.25 μL), and CD29 (0.625 μL) monoclonal antibodies (Santa Cruz Biotechnology, Inc., Santa Cruz, CA, USA). A blank control group was treated with an isotope antibody that had the same source and subgroup as the FITC-conjugated rat anti-mouse monoclonal antibodies. All samples were incubated at 4°C, washed, centrifuged at 1000 rpm for 5 min, and then resuspended in 200 μL of PBS. Flow cytometry was used to analyze the cells. Finally, the third-passage BMMSCs were used in all subsequent experiments.

SPION synthesis and labeling

The SPIO ($Fe^{3+}{}_2O_3M^{2+}O$; Southern Medical University, Guangzhou, China) used in this study was a 3-aminopropyl triethoxysilane-modified Fe_2O_3 particle with a diameter of 10-15 nm. The synthesis and phase transfer of SPIONs were performed according to published procedures [22]. Monodispersed SPIONs were first synthesized by thermal decomposition of iron oleate. SPION labeling of the BMSCs was performed as previously described. In brief, the hydrophilic SPIONs were sterilized by filtration through a 0.22-μm syringe filter into fresh DMEM/F-12; after which, poly-L-lysine (Gibco) was added to a final concentration of 0.75 μg/mL [23]. This was followed by homogenization for 60 min. Third passage BMSCs were washed three times with phosphate-buffered saline (PBS) and then grown in DMEM/F12 containing 10% FBS, 100 U/mL penicillin, and 100 ng/mL streptomycin. The cells were then incubated in 6-well plates with five different concentrations of SPIONs (0, 25, 50, 75 and 100 μg/mL) for 24 h at 37°C in a 5% CO_2 atmosphere with 95% humidity. At 24 h after labeling, the cells were subjected to Prussian blue iron (Beijing Leagene Biotech, Co., Ltd., Beijing, China) staining using Mallory's method [24]. The cells were then fixed in 4% paraformaldehyde for 30 min and rinsed three times with purified water. The reagent was mixed with an equal quantity of 2% hydrochloric acid and 2% potassium ferrocyanide, and then added to the cultures, followed by an overnight incubation. Images were taken with an inverted microscope (DMi1; Leica Microsystems GmbH, Wetzlar, Germany).

LPEMF exposure

The PEMF device (EBI, L.P. Parsippany, NJ, USA) was provided by the Department of Pathophysiology at Southern Medical University, and comprised a pulsed signal generator and Helmholz coils assembly with two-coils, operated by a spark gap pulse generator. The PEMF waveform used in the experiments consisted of a pulsed burst (pulse-width 360 ns, rise-time 10 ns, 400 kV/m) that was repeated at 50 Hz. When examining the effects of a LPEMF on SPION-labeled BMMSCs, the PEMF device was placed in a cell incubator (5% CO_2, 37°C). The BMMSCs were then seeded at different densities into tissue culture flasks using expansion medium. The cultures were placed into the PEMF device and exposed to the LPEMF for 3 h per day. The applied field consisted of 4.5 ms bursts of 20 pulses, repeating at 50 Hz. During each pulse, the magnetic field increased from 0 to 1.1 mT in 250 μs and then decayed back to 0 mT in 50 μs. An exposure apparatus with the same parameters had been used to significantly osteoblastogenesis in our previous studies. In order to perform control and experimental studies simultaneously, "sham irradiated" control samples were placed in another cell incubator with a properly energized actuator so as not to produce a PEMF stimulus, but ultimately generate the same quantity of heat as the actuator used in the experimental study. The temperatures were measured with a thermometer immediately before and after LPEMF stimulation. The cells were continuously cultured in a humid atmosphere with 5% CO_2 at 37°C throughout the course of each experiment.

CCK8 assay

To identify the safe concentration of SPIONs in BMMSCs, five groups of BMMSCs labeled with different concentrations of SPIONS (0, 25, 50, 75 and 100 μg/mL) were re-suspended at 2×10^4 cells/mL. These five experimental groups, together with a non-labeled control group, were seeded into 96-well plates (100 μL per well). After 24 h of culture, 10 μL of cell

Table 1. Random primer sequences used for the RT-PCR

Gene	Primer	Primer sequence (5'-3')	Product length
Runx2	F	TGCACCTACCAGCCTCACCATAC	105
	R	GACAGCGACTTCATTCGACTTCC	
ALP	F	GTTGCCAAGCTGGGAAGAACAC	121
	R	CCCACCCCGCTATTCCAAAC	
OCN	F	GGCGTCCTGGAAGCCAATGTG	132
	R	GACCAGGAGGACCAGGAAG TCCACGT	
β-actin	F	GCCAACACAGTGCTGTCT	114
	R	AGGAGCAATGATCTTGATCTT	

counting Kit-8 (CCK-8; Dojindo, Tokyo, Japan) reagent was added to each well; followed by an additional 2 h incubation. After incubation, the absorbance of each well at a 450 nm excitation wavelength was measured with a plate reader [25]. The cell growth inhibition caused by each concentration of SPIONs was calculated according to the following equation: inhibition rate = (O.D. control group - O.D. experimental group)/(O.D. control group - O.D. blank group) × 100. The optimum concentrations of SPIONS were used in the subsequent studies.

To study the proliferation of SPION-labeled BMMSCs in a LPEMF, BMMSCs labeled with 50 μg/mL SPIONS were placed into the wells of a 96-well plate and cultured in a specific growth medium starting at an initial density of 1×10^4 cells/mL (100 mL per well). The cells were incubated for at least 12 h to ensure sufficient adhesion. Next, the cells were continuously exposed to a 50 Hz, 1.1 mT LPEMF for 3 h each day, while the control group received sham exposure. After LPEMF stimulation, SPION-labeled BMMSC proliferation was quantified using a CCK-8 kit. A 20 mL volume of CCK-8 solution was added into each well of the plate. After incubation at 37°C for 2 h, the plate was shaken for 2 min on an oscillator; after which, a micro-plate reader was used to detect the OD value of each well at 450 nm. The same process was repeated for the next 9 days.

Directional migration analysis

SPION-labeled and non-labeled BMMSCs were seeded into ten culture flasks, which were then equally divided into experimental and control groups. Marked graduations were made to separate the bottom of each flack into two regions of equal size: an inner circle to indicate the central zone and an outer ring to indicate the peripheral zone. The experimental group cells were then placed under a 1.1 mT, 50 Hz LPEMF, and cell density was observed and photographed. Cell migration in the two groups was monitored by imaging the cell redistribution under influence of the LPEMF. After 3 h of LPEMF irradiation, images of the central and peripheral zones were taken via transmission electron microscopy. The total cell number in each flask was counted with a hemocytometer under a microscope. The experiments were repeated five times, independently.

At the same time, aliquots of BMMSCs were assigned to four different groups. Non-labeled BMMSCs without LPEMF exposure were administrated vehicle and served as a control group. Non-labeled BMMSCs stimulated with the LPEMF served as the second group. One group of SPION-labeled BMMSCs was exposed to a sham coil, while the other group of SPION-labeled BMMSCs was exposed to the LPEMF. Transwell assays were performed using Biocoat™ Matrigel™ Chambers with 8-μm pores (BD Biosciences, Franklin Lakes, NJ, USA) as described in the vendor's protocol. A total of 200 μL of serum-free RPMI medium containing 2×10^3 cells/mL (5×10^4 cells/well) was seeded into each upper chamber of the Transwell plate. The bottom chambers were filled with 1% fetal bovine serum-RPMI. The cells were then cultured at 37°C with 5% CO_2 for 48 h. Following culture, cells adhering to the membrane surface were fixed with 4% paraformaldehyde at room temperature for 30 min, permeabilized with 100% methanol for 20 min, and then stained with 1% crystal violet for 1 h. The membrane was then detached, wiped with a cotton swab, and examined under a microscope at ×100 magnification (Olympus, Tokyo, Japan). Three non-overlapping fields were chosen to calculate the total number of cells.

Von Kossa and ALP staining

Non-labeled BMMSCs (1×10^4 cells/mL) were seeded in four culture plates (A and B groups), and SPION-labeled BMMSCs were treated similarly (C and D groups). After the cells were cultured for 48 h, the medium was replaced with an osteogenic medium consisting of high-glucose DMEM (Gibco) supplemented with 10% FBS, 10 nmol/L dexamethasone (Sigma Aldrich, St. Louis, MO, USA), 10 mmol/L β-glycerol phosphate (Sigma Aldrich), and 50 μmol/L ascorbic

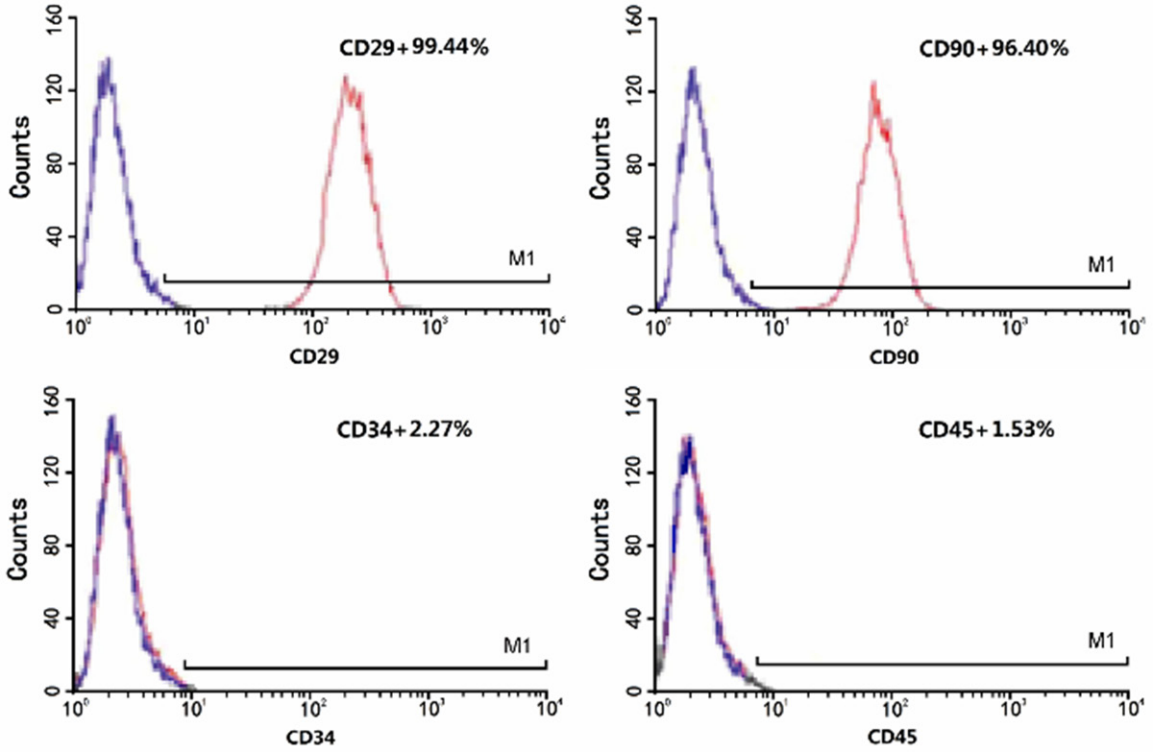

Figure 1. The expression levels of CD29, CD90, CD34, and CD45 in rat BMSCs were examined using flow cytometry. An isotype antibody served as a negative control (blue line). The percentages of CD29-positive and CD90-positive cells were 99.44% and 96.40%, respectively. The percentages of CD34-positive and CD45-positive cells were ~2.27% and 1.53%, respectively.

acid (Sigma Aldrich). The B and D groups were exposed to the 50 Hz, 1.1 mT LPEMF for 3 h each day, while the A and C groups were left untreated and served as controls. Von Kossa and ALP staining were performed 21 days later. After three washes with PBS, the cells were fixed with 4% paraformaldehyde for 30 min, soaked in an $AgNO_3$ solution, and then exposed to ultraviolet irradiation for 30 min. Next, the cells were rinsed with pure water, soaked in a sodium thiosulfate solution for 2 min, rinsed, and stained with dimethyl diaminophenazine chloride. Finally, the cells were dehydrated with ethanol and photographed [20] We also used a spectrophotometric method to evaluate ALP activity in the culture supernatants of the four groups [26].

Real-time PCR

After 21 days of osteogenic induction, four groups of BMMSCs were dissolved and their intracellular RNA was extracted and reverse transcribed using a Super-Script First Strand cDNA System (Invitrogen, Carlsbad, CA, USA). Primer sequences used for the RT-PCR are listed below (**Table 1**). The appropriate cDNA was synthesized for the real-time PCR, and the first strand cDNA products were amplified using PowerUp SYBR Green Master Mix (Stratagene, La Jolla, CA, USA) and specific primers as previously described [27]. The PCR conditions were 94°C for 45 s, 59°C for 45 s, and 72°C for 1 min. The relative mRNA expression levels were normalized to those for β-actin. Next, 1% agarose gel electrophoresis was used to analyze the PCR products and band intensity was quantitated using Image-Quant analysis software.

Western blotting

Four groups of BMMSCs were dissolved on ice, washed with ice-cold phosphate buffered saline (PBS), and subsequently immersed in RIPA buffer (1 × PBS, 1% NP40, 0.1% sodium dodecyl sulphate, 1 mM sodium orthovanadate, 0.5% sodium deoxycholate). The solutions were transferred to a microcentrifuge and stirred for 30 min at 4°C. Next, the cell lysates were centrifuged at 12,000 rpm for 10 min,

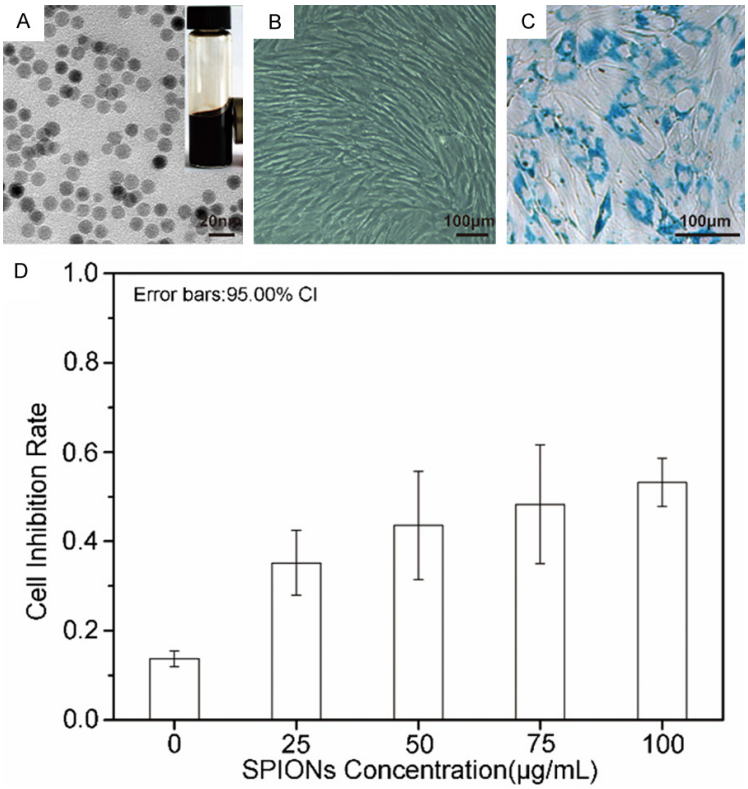

Figure 2. The effect of SPION on BMMSCs. A. TEM image of the synthesized 12 nm SPIONs. The inset shows a strong response of the nanoparticle solution to an external magnetic field. B. Third passage BMMSC morphology as viewed under a bright field microscope (×100 magnification). C. Prussian blue staining of BMMSCs incubated with 50 μg/mL SPIONs (×100 magnification). Inhibition of cell growth produced by exposure to different SPION concentrations for 6 consecutive days. Cell proliferation gradually decreased as the SPION concentration increased.

and the protein concentrations in the supernatants were measured with the Bradford protein assay (Bio-Rad Laboratories, Hercules, CA, USA). The supernatant proteins were separated by SDS-PAGE and then electrophoretically transferred (16 V for 2 h) onto polyvinylidene difluoride (PVDF) membranes (Amersham Pharmacia Biotech, Piscataway, NJ, USA) using a transfer buffer (25 mM Tris, 192 mM glycine, 4% methanol, pH 8.3). The membranes were blocked with 5% (w/v) defatted milk. Murine monoclonal antibodies Runx2 (1:1000), OCN (1:1000), ALP (1:1000), and β-actin (1:3000, Abcam, UK) were added to the membranes and incubated overnight at 4°C. The membranes were then washed with PBS, and horseradish peroxidase-conjugated anti-mouse secondary antibody (1:5000 dilution in TBS, Abcam) was administrated for 60 min at room temperature. Immunostaining was detected using an ECL Plus western blotting analysis system (Pierce, Rockford, IL, USA). The luminescent signals were recorded with BioMax X-ray film (Amersham Biosciences, UK). β-actin was used an internal control to confirm the equal loading of proteins. Each well of the plate was considered as an individual sample. At least 3 independent experiments were performed in succession.

Statistical analysis

All numerical results represent the mean ± standard deviation. ALP activity in the four groups was compared by one-way analysis of variance (ANOVA). Repeated measures ANOVA was used to check the cell density of various regions before and after LPEMF irradiation. A P-value < 0.05 was considered statistically significant. All statistical analyses were performed using SPSS for Windows, Version 13.0.

Results

Purification of BMMSCs

In the present study, BMMSCs were isolated from the tibias and fibulas of rats and then cultured *ex vivo*. Primary BMMSCs were continuously passaged into the third generation. Flow cytometry analyses showed that surface markers CD29 and CD90 were present in 99.44% and 96.40% of cells, respectively. The hematopoietic stem cell markers CD34 and CD45 were present in 2.27% and 1.53% of cells, respectively (**Figure 1**).

SPION labeling of BMMSCs

Monodispersed SPIONs were synthesized by thermal decomposition of iron oleate as previously described [28]. TEM observations showed the nanoparticles were ~12 nm in diameter (**Figure 2A**). The nanoparticles had a strong saturated magnetic moment. Their aqueous solution behaved similar to a ferrofluid (**Figure 2A**, inset) and responded to the magnetic field of a handheld magnet. Long spindle-and polygonal-shaped third-passage rat BMMSCs were confirmed by flow cytometric analysis as described above. These cells grew on the cul-

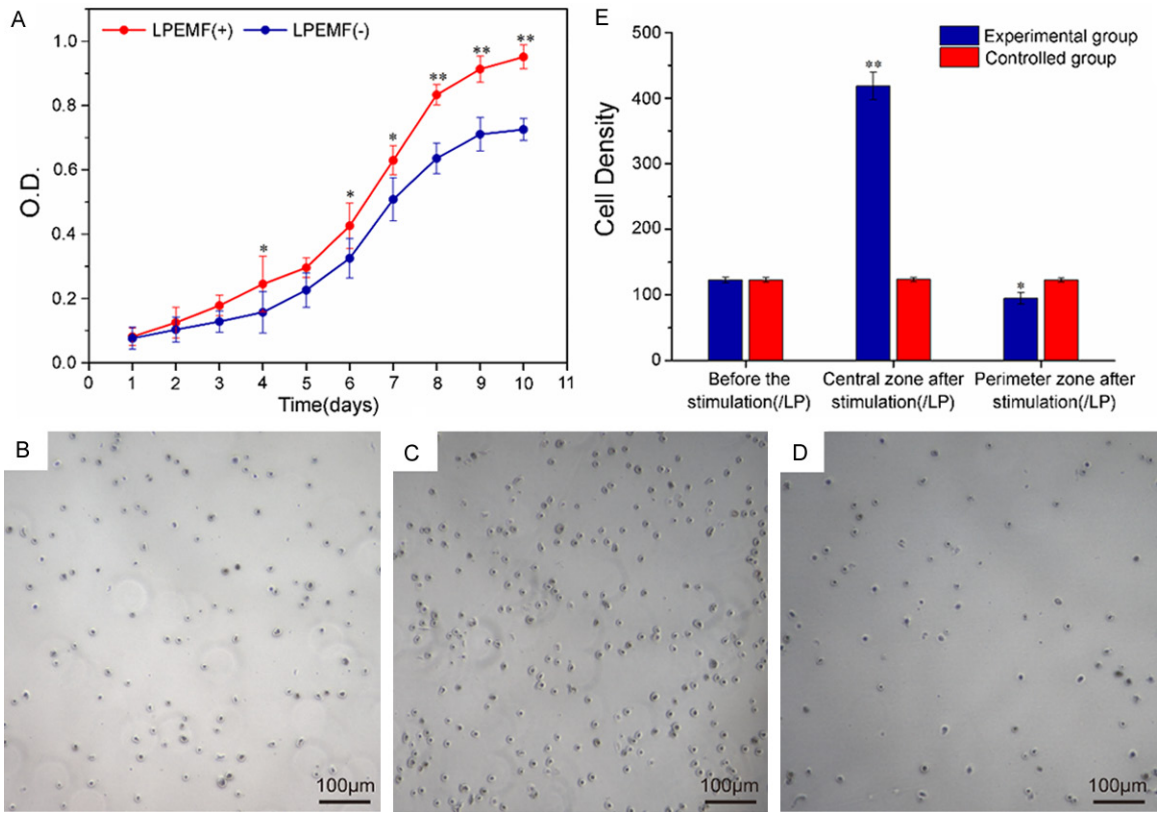

Figure 3. Cell performance on cell growth, cell density and distribution after stimulated by LPEMF. A. Cell growth curves of 50 μg/mL SPION-labeled BMMSCs with or without exposure to the LPEMF. B. Cells were uniformly distributed prior to application of the LPEMF. C. Cells aggregated after 2 h of LPEMF exposure. D. Cells were much sparser in the peripheral zone where the LPEMF wasn't applied. Scale bar = 100 μm. E. Cell density in the different zones before and after LPEMF stimulation. *P < 0.05 compared with cell density before stimulation. **P < 0.01 compared with cell density before stimulation. Data are presented as the mean ± SD (n = 3). *P < 0.05 and **P < 0.01 compared with the LPEMF(-) group.

ture substrates in a spiral arrangement as observed under a light microscope (**Figure 2B**). Loading of SPIONs onto BMMSCs was confirmed by Prussian blue staining. The SPIONs were stained blue and scattered around the cell nuclei (**Figure 2C**). The percentage of cells labeled with SPIONs reached 100% when they were incubated with a SPION solution ≥ 50 μg/mL. However, the cells showed relatively light Prussian blue staining when they were incubated with 25 μg/mL SPIONs, indicating that 25 μg of SPIONs was insufficient to label all of the cells.

In vitro safety evaluation of SPIONS in BMMSCs

As shown in **Figure 2D**, cell proliferation gradually decreased as the SPION concentration increased. While cells in the 25 μg SPION/mL group showed the lowest proliferation rate, the rate was not significantly different from that in the 50 μg SPION/mL group. ($P = 0.076$). Given that a SPION concentration of 25 μg/mL was insufficient to label all of the cells (as mentioned above), we used the 50 μg SPION/mL concentration when conducting our subsequent experiments.

LPEMF significantly promoted the proliferation of SPION-labeled BMMSCs

It was previously demonstrated that a 50 Hz LPEMF could promote the proliferation of BMMSCs [29]. In our study, the O.D. value of the cultured cells was measured for 10 consecutive days. After 4 days of culture, the O.D. value of the non-treated control group increased from 0.076 to 0.157, while that of the experimental irradiated group increased from

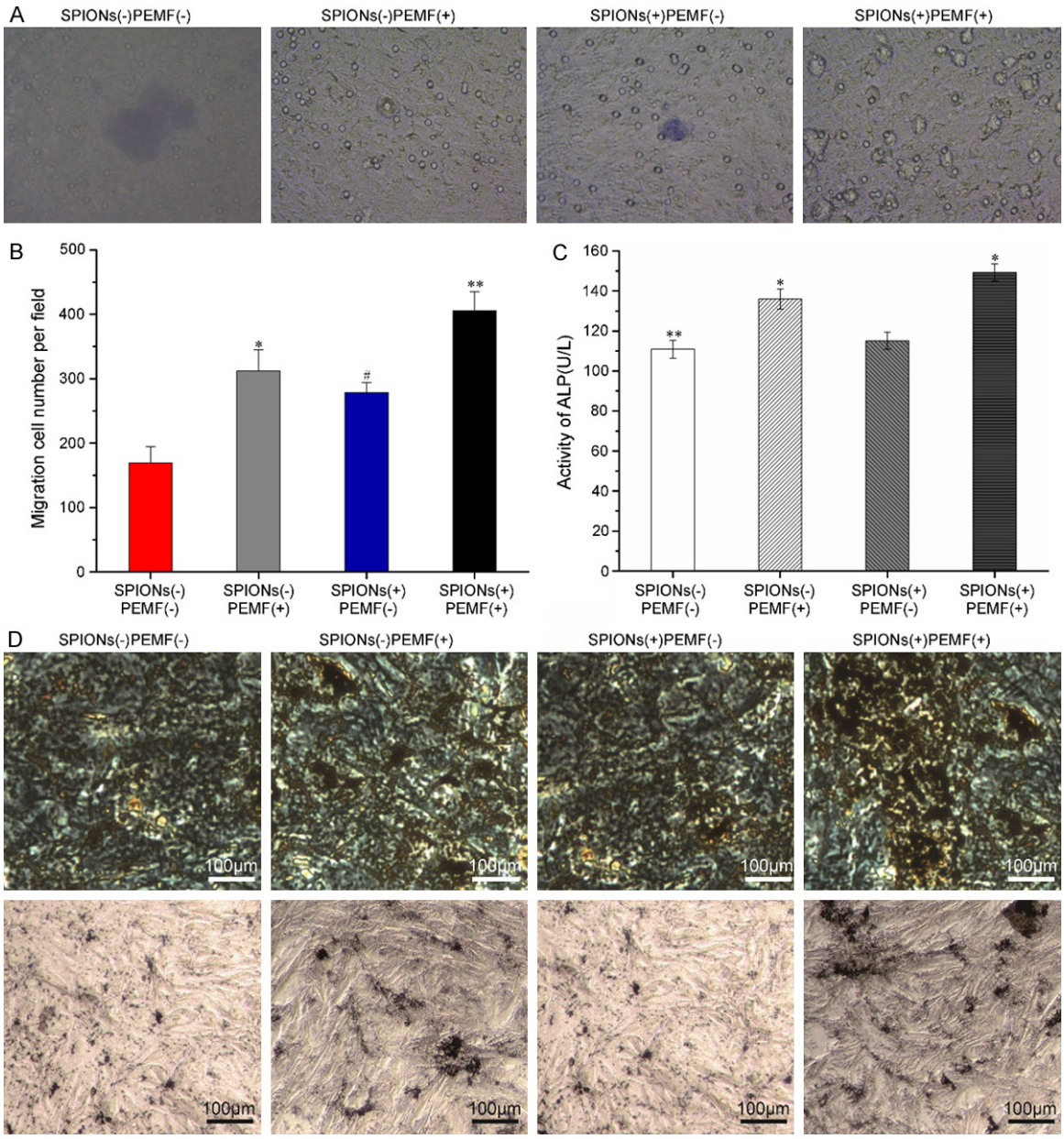

Figure 4. Effect of SPIONs and PEMF on Cell migration, von Kossa calcim staning, activity of ALP of BMMSCs. A and B. Transwell experiments showed that the number of migrating BMMSCs in the LPEMF(+)SPION(+) group was significantly greater than those numbers in the other three groups. *P < 0.05, **P < 0.01, #P > 0.05 compared with the control group. C. ALP activity in the four BMSC groups after 21 days of osteogenic induction. *P < 0.01 compared with any other group. D. (Top row) von Kossa calcium staining and (bottom row) ALP staining of the four BMMSC groups after 21 days of osteogenic induction. Visible black crystalline mineral deposits were observed after staining. Combined SPION labeling plus LPEMF exposure.

0.081 to 0.245. There was an obvious increase in the number of cells when compared with the sham exposure group, and this growth trend remained constant during the following 6 days. (**Figure 3A**) These data demonstrated that a LPEMF could significantly promote the proliferation of BMMSCs labeled with SPIONs.

SPION-labeled BMMSCs migrated directionally toward the LPEMF

Before the LPEMF was applied, the two groups of cells were uniformly distributed in the field of view (**Figure 3B**). After 2 h of LPEMF exposure, the concentration SPION-labeled cells in the

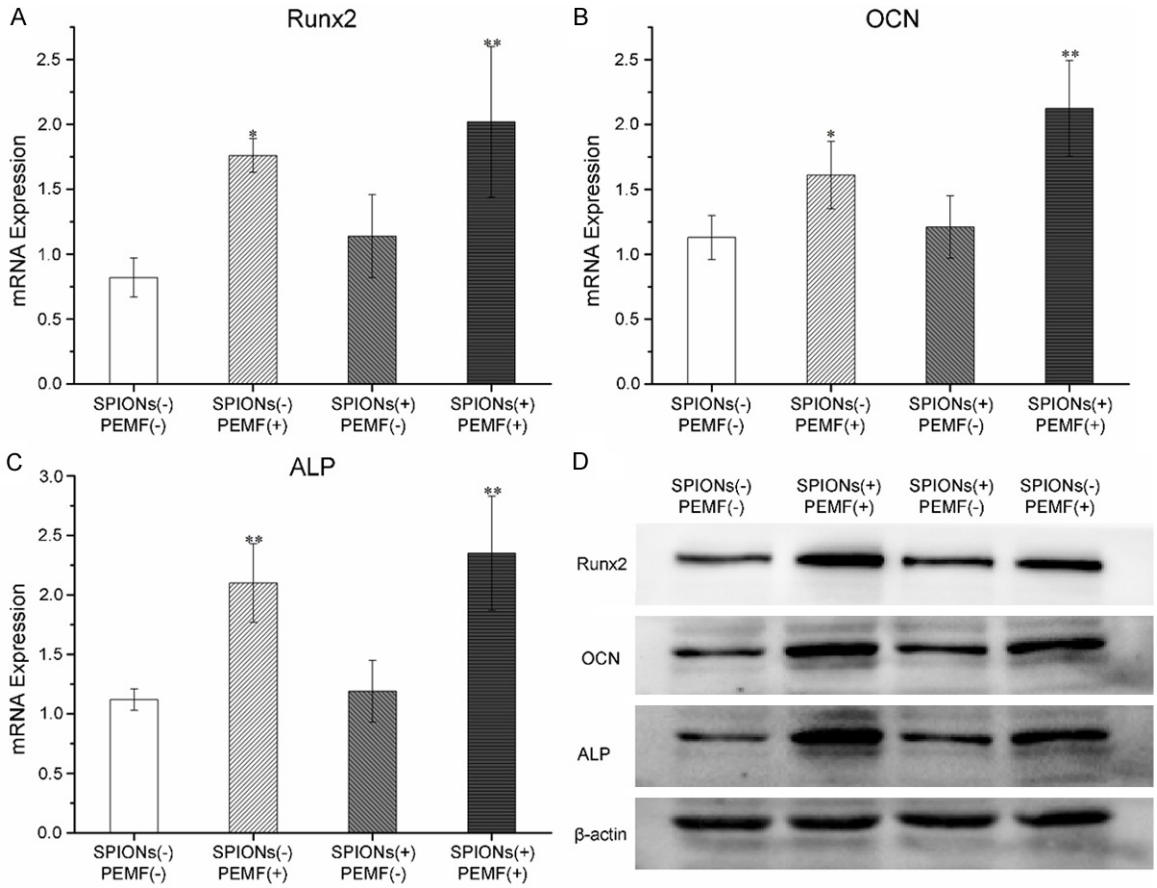

Figure 5. Expression of Runx2, OCN and ALP after 21 days of osteogenic induction. The qRT-PCR analyses showed that LPEMF exposure significantly increased the expression of genes related to cell differentiation in SPION-labeled cells. Data acquired by the RT-PCR assays are presented as the mean ± SD (n = 3). The relative expression level of each gene was normalized to that of β-actin, and the ratio is given. *P < 0.05, **P < 0.01 compared with the SPION(-)PEMF(-) group. Expression of osteoblastogenesis-related proteins after 21 days of osteogenic induction. Western blot studies showed that LPEMF exposure significantly increased the synthesis of osteoblastogenesis-related proteins in SPIONs-labeled cells. Relative protein content was normalized to that of β-actin.

central area of the magnetic field increased substantially (**Figure 3C**), while the concentration of cells in the peripheral zone without LPEMF stimulation decreased (**Figure 3D**). The effect of the LPEMF on cell density was statistically significant when analyzed by repeated measures ANOVA (**Figure 3E**). Non-labeled BMMSCs did not show a significant difference of cell density in the central zone when compared with that in the peripheral zone, indicating that the observed increase in cell density under influence of the LPEMF was due to cell migration rather than cell proliferation.

Transwell assay results showed that the number of cells passing through the Transwell chamber was much higher in the group with LPEMF exposure than in the sham exposure group. Moreover, the maximum migratory effect was observed in the group in which the cells were labeled with SPIONs and also exposed to the LPEMF (**Figure 4A**). The number of migrated cells in each group was counted and analyzed. The results showed that there were more cells migrating into the lower Transwell chamber in the SPION(+)PEMF(+) group, when compared with the control group (**Figure 4B**). These results suggested that the combination of SPION-labeling plus LPEMF exposure significantly promoted the directional migration of BMMSCs.

The LPEMF and SPIONs synergistically promoted the osteoblastic differentiation of BMMSCs

The individual and combined effects of the LPEMF and SPIONs were investigated by observing changes in cell morphology, bone for-

mation, and ALP activity in four parallel cultures. As shown by the results of von Kossa staining and ALP staining (**Figure 4D**), all four cultures displayed osteogenic activity; however, the cells labeled with SPIONs and also exposed to the LPEMF differentiated more rapidly than cells in the other cultures. Furthermore, our results showed that exposure to the LPEMF alone was sufficient to promote cell differentiation when compared with non-treated cells, regardless of whether the cells were labeled with SPIONs or not. SPION-labeled cells that were not exposed to the LPEMF did not show any differences in terms of bone formation when compared with non-labeled cells. This demonstrated that SPIONs alone do not promote differentiation. We found that the ALP activity of SPION-labeled cells with LPEMF stimulation was significantly higher than that of the other groups ($P < 0.001$). Similarly, LPEMF exposure alone was sufficient to increase cellular ALP activity, regardless of whether the cells were labeled with SPIONs (**Figure 4C**).

The synergistic effect of LPEMF exposure and SPIONs on promoting BMMSC osteoblastic differentiation was detected via RT-PCR and western blotting. SPION-labeled and non-labeled BMMSCs were transferred into a 6-well cell culture plate containing osteogenesis inductive medium at a density of 2×10^5 cells/mL (2 mL per well). After LPEMF exposure (1.1 mT, 3 h/day) for 21 days, the levels of Runx2, OCN, ALP, and β-actin expression were measured using RT-PCR. The results showed that when compared with the control group, LPEMF stimulation greatly promoted the expression of osteogenesis-related genes in SPION-labeled BMMSCs. At the same time, Runx2, OCN, and ALP expression were also significantly enhanced in the PEMF(+)SPION(-) group, but not as much as in the PEMF(+)SPION(+) group (**Figure 5A-C**).

The levels of osteoblastogenesis-related protein expression as detected in western blot studies are shown in **Figure 4D**. The levels of Runx2, OCN, and ALP expression were significantly higher in the LPEMF group than in the group without LPEMF stimulation, regardless of whether the cells were labeled. However, there were no differences between the osteoblastogenesis-related proteins expressed by the SPION-labeled cells and non-labeled cells. The overall level of osteoblastogenesis-related protein expression in the PEMF(+)SPION(°C) group was significantly higher than that in the other groups. When taken together, the above results indicated that the combined effect of the LPEMF plus SPIONs was stronger than that of either factor applied alone, indicating a synergistic effect of SPIONs and a LPEMF on the osteoblastic differentiation of BMMSCs.

Discussion

In recent decades, pulsed electromagnetic fields have been shown to exert biological effects in treating bone defect disorders, and especially fractures, osteoporosis, and bone nonunion [30, 31]. Some studies have revealed that different cell types display higher degrees of proliferation and differentiation after PEMF exposure [32, 33]. These findings suggest that a PEMF might influence the osteoblastogenesis process. Our recently research showed that SPION-labeled osteoblasts could affect bone structure and function and increase trabecular bone mass and strength (data not shown). It has been suggested that magnetic fields activate the superparamagnetism of SPIONs, which enables them to promote the differentiation of bone progenitor cells into osteoblasts. However, few studies have reported the use of a PEMF in targeted therapy. In this study, we constructed a model of bone marrow mesenchymal cells, and then labeled them with SPIONs. The effect of a PEMF on the SPION-labeled BMMSCs was then investigated.

Previous studies explored the safety of using SPIONs for clinical purposes. Wang et al. [34] added iron oxide nanoparticles (IONs) to mesenchymal stem cells, and showed that ION labeling did not induce apoptosis. We obtained similar results in this study. Although there was a dose-dependent effect of SPION concentration on cell proliferation, the concentrations needed to label the majority of cells (25 and 50 μg/mL) had negligible effects on cell growth. However, a 50 μg/mL SPION concentration was determined to be the optimal concentration due to its complete labeling capability and low cytotoxicity.

Previous studies confirmed that a LPEMF could increase BMMSC proliferation by 29.6% when compared with non-treated cells [29, 35]. However, few studies have reported the effect

of a LPEMF on the proliferation of SPION-labeled BMMSCs. We generated a cell growth curve and found that after 4 days of culture, the O.D. value of SPIONs-labeled cells treated with a LPEMF increased by 2-fold when compared with that of SPION-labeled cells without LPEMF exposure. Furthermore, that growth trend remained constant during the subsequent 6 days, demonstrating that the LPEMF had significantly promoted the proliferation of BMMSCs labeled with 50 μg/mL SPIONs.

Artificial control of the direction that stem cells move is a key study point of targeted therapies based on stem cells and nanomaterials. This area requires studying directional migration *in vitro* and targeted uptake in an *in vivo* microenvironment, as well as the proliferation and differentiation of stem cells and their biological safety. Endogenous and exogenous BMMSCs migrate from the blood through vascular endothelial cells under the influence of a variety of factors. They reach their target tissue for colonization and retain their differentiation potential via a process known as BMMSC "homing" [36]. Similar to the cardiovascular system, a LPEMF can deeply penetrate human tissue and guide ferromagnetic particles such as SPIONs to their target tissues [37]. Our findings showed that LPEMF exposure for 3 h/day increased the density of labeled cells, rather than unlabeled cells, in the central region where the LPEMF was applied ($P < 0.001$), indicating that SPION-labeled BMMSCs could directionally migrate *in vitro* under stimulation of a LPEMF. This finding suggests that stem cell movement can be controlled by this system, and encourages further studies of the targeted uptake of BMMSCs in an *in vivo* microenvironment.

Kanczler et al. [28] applied a remote magnetic field to activate nanoparticle mechanoreceptors adhered to BMMSCs. This application resulted in bone progenitor differentiation *in vitro*, and apparent increases in the synthesis of proteoglycans, type I and II collagen, and extracellular matrix. Therefore, we hypothesized that osteogenic differentiation might be enhanced by applying SPION-labelled BMMSCs capable of functioning under the influence of a LPEMF. In our study, we found that SPION-labeled BMMSCs exposed to a LPEMF not only differentiated more rapidly than other groups of cells, but also displayed the strongest von Kossa and ALP staining, the most abundant black crystalline minerals, and the highest ALP activity. We also found that SPION-labeled BMMSCs with LPEMF exposure exhibited the highest levels of osteogenesis-related gene and protein expression when compared with the other groups. These results strongly suggest that a LPEMF combined with SPIONs synergistically promotes the osteogenic differentiation of BMMSCs.

Conclusion

Given that a SPION is a new nanomaterial without much biological activity, it may be surprising that cells labeled with SPIONs have an enhanced osteogenesis potential, especially during exposure to a LPEMF. Our present studies showed that the proliferation of SPION-labeled cells can be promoted by exposure to a LPEMF, and also revealed a significant synergistic effect on *in-vitro* osteoblast differentiation. Furthermore, we discovered the directional migration of SPION-labeled BMMSCs *in vitro*, which serves as a good reference for related studies and lays the foundation for further *in vivo* experimentation. However, some challenging issues remain to be solved, including how to promote the homing of composite particles, improve the biological compatibility of nanomaterials, further reduce cytotoxicity, and improve the targeting efficiency of labeled cells. Nonethe-less, our results still provide an important foundation for further exploration, and suggest new directions for bone fracture and bone defect therapies.

Disclosure of conflict of interest

None.

Address correspondence to: Dr. Jing Tian, Department of Orthopedics, Zhujiang Hospital, Southern Medical University, NO. 253 Industrial Avenue, Haizhu District, Guangzhou 510280, Guangdong, PR China. Tel: 00862061643010; Fax: 00862061-643010; E-mail: tianjing_ortho@163.com

References

[1] Reid I. Anti-resorptive therapies for osteoporosis. Semin Cell Dev Biol 2008; 19: 473-478.
[2] Brommage R. Genetic approaches to identifying novel osteoporosis drug targets. J Cell Biochem 2015; 116: 2139-2145.

[3] Fulfaro F, Casuccio A, Ticozzi C and Ripamonti C. The role of bisphosphonates in the treatment of painful metastatic bone disease: a review of phase III trials. Pain 1998; 78: 157-169.
[4] Turgeon JL, McDonnell DP, Martin KA and Wise PM. Hormone therapy: physiological complexity belies therapeutic simplicity. Science 2004; 304: 1269-1273.
[5] Li X, Zhang M, Bai L, Bai W, Xu W and Zhu H. Effects of 50 Hz pulsed electromagnetic fields on the growth and cell cycle arrest of mesenchymal stem cells: an in vitro study. Electromagn Biol Med 2012; 31: 356-364.
[6] Li S, Luo Q, Huang L, Hu Y, Xia Q and He C. Effects of pulsed electromagnetic fields on cartilage apoptosis signalling pathways in ovariectomised rats. Int Orthop 2011; 35: 1875-1882.
[7] Chalidis B, Sachinis N, Assiotis A and Maccauro G. Stimulation of bone formation and fracture healing with pulsed electromagnetic fields: biologic responses and clinical implications. Int J Immunopathol Pharmacol 2011; 24: 17-20.
[8] Assiotis A, Sachinis NP and Chalidis BE. Pulsed electromagnetic fields for the treatment of tibial delayed unions and nonunions. A prospective clinical study and review of the literature. J Orthop Surg Res 2012; 7: 24.
[9] Ding S, Peng H, Fang HS, Zhou JL and Wang Z. Pulsed electromagnetic fields stimulation prevents steroid-induced osteonecrosis in rats. BMC Musculoskelet Disord 2011; 12: 215.
[10] Teven CM, Greives M, Natale RB, Su Y, Luo Q, He BC, Shenaq D, He TC and Reid RR. Differentiation of osteoprogenitor cells is induced by high-frequency pulsed electromagnetic fields. J Craniofac Surg 2012; 23: 586-593.
[11] Loughran JH, Chugh AR, Ismail I and Bolli R. Stem cell therapy: promising treatment in heart failure? Curr Heart Fail Rep 2013; 10: 73-80.
[12] Palumbo R, Sampaolesi M, De Marchis F, Tonlorenzi R, Colombetti S, Mondino A, Cossu G and Bianchi ME. Extracellular HMGB1, a signal of tissue damage, induces mesoangioblast migration and proliferation. J Cell Biol 2004; 164: 441-449.
[13] Wecht S and Rojas M. Mesenchymal stem cells in the treatment of chronic lung disease. Respirology 2016; 21: 1366-1375.
[14] Wang C, Meng H, Wang X, Zhao C, Peng J and Wang Y. Differentiation of bone marrow mesenchymal stem cells in osteoblasts and adipocytes and its role in treatment of osteoporosis. Med Sci Monit 2016; 22: 226-233.
[15] Kumar S, Wan C, Ramaswamy G, Clemens TL and Ponnazhagan S. Mesenchymal stem cells expressing osteogenic and angiogenic factors synergistically enhance bone formation in a mouse model of segmental bone defect. Mol Ther 2010; 18: 1026-1034.
[16] Chen Y, Jiang P, Liu S, Zhao H, Cui Y and Qin S. Purification of 6xHis-tagged phycobiliprotein using zinc-decorated silica-coated magnetic nanoparticles. J Chromatogr B Analyt Technol Biomed Life Sci 2011; 879: 993-997.
[17] Chekman IS, Ulberg ZR, Gorchakova NO, Nebesna TY, Gruzina TG, Priskoka AO, Doroshenko AM and Simonov PV. The prospects of medical application of metal-based nanoparticles and nanomaterials. Lik Sprava 2011; 3-21.
[18] Swiston AJ, Cheng C, Um SH, Irvine DJ, Cohen RE and Rubner MF. Surface functionalization of living cells with multilayer patches. Nano Lett 2008; 8: 4446-4453.
[19] Bakhtiary Z, Saei AA, Hajipour MJ, Raoufi M, Vermesh O and Mahmoudi M. Targeted superparamagnetic iron oxide nanoparticles for early detection of cancer: possibilities and challenges. Nanomedicine 2016; 12: 287-307.
[20] Singh R and Lillard JW Jr. Nanoparticle-based targeted drug delivery. Exp Mol Pathol 2009; 86: 215-223.
[21] Jiang J, Gu H, Shao H, Devlin E, Papaefthymiou GC and Ying JY. Bifunctional Fe_3O_4-Ag heterodimer nanoparticles for two-photon fluorescence imaging and magnetic manipulation. Advanced Materials 2010; 20: 4403-4407.
[22] Jansen JH, van der Jagt OP, Punt BJ, Verhaar JA, van Leeuwen JP, Weinans H and Jahr H. Stimulation of osteogenic differentiation in human osteoprogenitor cells by pulsed electromagnetic fields: an in vitro study. BMC Musculoskelet Disord 2010; 11: 188.
[23] Neri M, Maderna C, Cavazzin C, Deiddavigoriti V, Politi LS, Scotti G, Marzola P, Sbarbati A, Vescovi AL and Gritti A. Efficient in vitro labeling of human neural precursor cells with superparamagnetic iron oxide particles: relevance for in vivo cell tracking. Stem Cells 2008; 26: 505-516.
[24] Fathima H and Harish. Osteostimulatory effect of bone grafts on fibroblast cultures. J Nat Sci Biol Med 2015; 6: 291-294.
[25] Zeng G, Wang G, Guan F, Chang K, Jiao H, Gao W, Xi S and Yang B. Human amniotic membrane-derived mesenchymal stem cells labeled with superparamagnetic iron oxide nanoparticles: the effect on neuron-like differentiation in vitro. Mol Cell Biochem 2011; 357: 331-341.
[26] Hansen HA and Weinfeld A. Hemosiderin estimations and sideroblast counts in the differential diagnosis of iron deficiency and other anemias. Acta Med Scand 1959; 165: 333-356.
[27] Zhai M, Jing D, Tong S, Wu Y, Wang P, Zeng Z, Shen G, Wang X, Xu Q and Luo E. Pulsed elec-

tromagnetic fields promote in vitro osteoblastogenesis through a Wnt/beta-catenin signaling-associated mechanism. Bioelectromagnetics 2016; [Epub ahead of print].

[28] Kanczler JM, Sura HS, Magnay J, Green D, Oreffo RO, Dobson JP and El Haj AJ. Controlled differentiation of human bone marrow stromal cells using magnetic nanoparticle technology. Tissue Eng Part A 2010; 16: 3241-3250.

[29] Sun LY, Hsieh DK, Lin PC, Chiu HT and Chiou TW. Pulsed electromagnetic fields accelerate proliferation and osteogenic gene expression in human bone marrow mesenchymal stem cells during osteogenic differentiation. Bioelectromagnetics 2010; 31: 209-219.

[30] Osti L, Buono AD and Maffulli N. Pulsed electromagnetic fields after rotator cuff repair: a randomized, controlled study. Orthopedics 2015; 38: e223-228.

[31] Jing D, Zhai M, Tong S, Xu F, Cai J, Shen G, Wu Y, Li X, Xie K, Liu J, Xu Q and Luo E. Pulsed electromagnetic fields promote osteogenesis and osseointegration of porous titanium implants in bone defect repair through a Wnt/beta-catenin signaling-associated mechanism. Sci Rep 2016; 6: 32045.

[32] Jing D, Cai J, Wu Y, Shen G, Li F, Xu Q, Xie K, Tang C, Liu J, Guo W, Wu X, Jiang M and Luo E. Pulsed electromagnetic fields partially preserve bone mass, microarchitecture, and strength by promoting bone formation in hindlimb-suspended rats. J Bone Miner Res 2014; 29: 2250-2261.

[33] Fredericks DC, Nepola JV, Baker JT, Abbott J and Simon B. Effects of pulsed electromagnetic fields on bone healing in a rabbit tibial osteotomy model. J Orthop Trauma 2000; 14: 93-100.

[34] Wang Y, Wang Y, Wang L, Che Y, Li Z and Kong D. Preparation and evaluation of magnetic nanoparticles for cell labeling. J Nanosci Nanotechnol 2011; 11: 3749-3756.

[35] Sun LY, Hsieh DK, Yu TC, Chiu HT, Lu SF, Luo GH, Kuo TK, Lee OK and Chiou TW. Effect of pulsed electromagnetic field on the proliferation and differentiation potential of human bone marrow mesenchymal stem cells. Bioelectromagnetics 2009; 30: 251-260.

[36] Wang Y, Deng Y and Zhou GQ. SDF-1alpha/CXCR4-mediated migration of systemically transplanted bone marrow stromal cells towards ischemic brain lesion in a rat model. Brain Res 2008; 1195: 104-112.

[37] Breathnach CS. Magnetism in medicine. Ir Med J 1983; 76: 337.